Ab initio and DFT studies on 1-(thionitrosomethylene) hydrazine: Conformers, energies, and intramolecular hydrogen-bond strength

ARTICLE *in* STRUCTURAL CHEMISTRY · AUGUST 2013

Impact Factor: 1.84 · DOI: 10.1007/s11224-012-0144-6

4 AUTHORS, INCLUDING:

Mehdi Yoosefian
Kerman Graduate University of Technology
42 PUBLICATIONS **284** CITATIONS
SEE PROFILE

Fariba Mollania
University of Birjand
24 PUBLICATIONS **101** CITATIONS
SEE PROFILE

Struct Chem
DOI 10.1007/s11224-012-0144-6

ORIGINAL RESEARCH

Ab initio and DFT studies on 1-(thionitrosomethylene) hydrazine: conformers, energies, and intramolecular hydrogen-bond strength

Heidar Raissi · Azadeh Khanmohammadi · Mehdi Yoosefian · Fariba Mollania

Received: 21 June 2012 / Accepted: 24 September 2012

Abstract In the current study, we present an intramolecular HB, molecular structure, π-electrons delocalization and vibrational frequencies analysis of 25 possible conformers of 1-(thionitrosomethylene) hydrazine by means of DFT (B3LYP), MP2 methods in conjunction with the 6-311++G** and augmented correlation-consistent polarized-valence triple-zeta basis sets and G2MP2 theoretical level. The influence of the solvent on the stability order of conformers and the strength of intramolecular hydrogen-bonding was considered using the Tomasi's polarized continuum model. Statistical analyses of quantitative definitions of aromaticity, nucleus independent chemical shift, harmonic oscillator model of aromaticity, aromatic fluctuation index, and the π-electron delocalization parameter (Q) as a geometrical indicator of a local aromaticity, evaluated for this conformers. Further verification of the obtained transition state structures were implemented via intrinsic reaction coordinate (IRC) analysis. Calculations of the ^{1}H NMR chemical shift at GIAO/B3LYP/6-311++G** levels of theory are also presented. The calculated highest occupied molecular orbital (MO) and lowest unoccupied MO energies show that charge transfer occur within the molecule. Hydrogen-bond energies for H-bonded conformers were obtained from Espinosa method and the natural bond orbital theory and the atoms in molecules theory were also applied to get a more precise insight into the nature of such H-bond interactions.

H. Raissi (✉) · A. Khanmohammadi · M. Yoosefian (✉) · F. Mollania
Chemistry Department, Birjand University, Birjand, Iran
e-mail: hraissy@yahoo.com

M. Yoosefian
e-mail: myoosefian@yahoo.com

Keywords 1-(Thionitrosomethylene) hydrazine · Intramolecular HB · Aromaticity indices · HOMO and LUMO · AIM and NBO

Introduction

Hydrazine is an important inorganic chemical with high heats of combustion and hence becomes highly useful as rocket fuel. Hydrazine and its derivatives are widely used in agricultural chemicals (pesticides), chemical blowing agents, pharmaceutical intermediates, photography chemicals, and boiler water treatment in hot-water heating systems for corrosion control [1]. It is also very important in pharmacology, because it is recognized as a carcinogenic, hepatotoxic, and mutagenic substance [2, 3]. It has been reported that hydrazine and its derivatives have adverse health effects [4]. Therefore, sensitive detection of hydrazine is practically important for environmental and biological analysis [5]. Further, hydrazine and water are highly polar by nature and between them there is strong hydrogen-bonding. Hydrogen-bonds are a key aspect of molecular structure and the subject of a vast number of theoretical and experimental studies. The investigation of hydrogen-bond is a crucial issue in the study of biologically active molecules, because it influences molecular properties and behavior, including biological and pharmacological activities [6, 7] e.g., the antioxidant and antiradical activities of some compounds. The properties of hydrogen-bonds X–H···Y are not only dependent on the properties of X, Y, and H but also are related to other factors such as substituent, hybridization, and solvation [8–16]. The chemical phenomenon of hydrogen-bonding has also been studied extensively by quantum-mechanical ab initio calculations [17, 18]. Changes in the electron

Published online: 07 October 2012

density distribution in both the donor and acceptor molecules are one of the consequences of hydrogen-bond formation. Thus, the change of electron density on the hydrogen acceptor changes the strength of hydrogen-bond.

Gilli et al. [19–21] have proposed the RAHB model to link the strength of the hydrogen-bonding to the resonance in chelated systems. In RAHB, the hydrogen-bond donor and acceptor atoms are connected through π-conjugated double bonds, which were utilized in this study.

1-(Thionitrosomethylene) hydrazine (TNMH) is an interesting molecule that possesses three types of intramolecular HBs, S–H···N, N–H···S, and N–H···N. Theoretically three classes of tautomers, Tiol-Imine (TI-I), Tio-Amine (T-A), and Tio-Imine (T-I) can be expected for it (see Fig. 1). In this investigation, the approximate values of the intramolecular HB energies were estimated by the Espinosa and Molins method [22].

The aim of this study is the prediction of the most stable structure among the equilibrium conformations in the gas phase and in solution, and evaluation of the intramolecular HB energy in chelated forms.

Details of the calculations

Ab initio and DFT calculations were carried out using the Gaussian 98 program [23]. The relative energies were calculated at the B3LYP [24] and the extrapolated MP2 (including the second-order correlation corrections) [25] methods with 6-311++G** basis set and G2MP2 theoretical level. The obtained structures then reoptimized at B3LYP and MP2 levels of theory with the augmented correlation-consistent polarized-valence triple-zeta (aug-cc-pVTZ) basis set [26] to find the minimum energy structure.

Harmonic vibrational frequencies were estimated at the same levels to confirm the nature of the stationary points found and also to account for the zero point vibrational energy (ZPVE) correction. The nature of the intramolecular HB in TNMH conformers have been studied using the atoms in molecules (AIM) theory of Bader by means of AIM 2000 [27] software using the B3LYP/6-311++G** wave functions as input. Natural bond orbital (NBO) analysis [28] at the same level of DFT theory was carried out to understand the orbital interactions and charge delocalization during the course of the reaction. The contour plot for visualization of the NBO result is constructed on NBOView (Version1.1) [29] software package using the standard keywords implemented therein. The actual calculations were performed for two solvent (CCl_4 and water), which were modeled using the polarizable continuum model (PCM) [30]. The PCM uses the united atom cavity approach. Cavity parameters used in all calculations were $O_{Fac} = 0.89$ (overlap index between two interlocking spheres) and $R_{Min} = 0.2$ (minimum radius in Angstroms for overlapping spheres). On the other hand, the aromaticity of the ring formed is measured using several well-established indices of aromaticity such as the nucleus independent chemical shift (NICS) [31], the harmonic oscillator model of aromaticity (HOMA) [32], and the para-delocalization index (PDI) [33], as well as a recently defined descriptor of aromaticity: the aromatic fluctuation index (FLU) [34]. In the present study, the R_{opt}, α and δ_{ref} parameters for HOMA and FLU indices were calculated at the B3LYP/6-311++G** level (for CN, NN, and NS bonds: $R_{opt,CN} = 1.333$ Å, $R_{opt,NN} = 1.318$ Å, $R_{opt,NS} = 1.630$ Å, $\alpha_{CN} = 91.61$, $\alpha_{NN} = 60.93$, $\alpha_{NS} = 136.63$, $\delta_{ref\ CN} = 1.32$, $\delta_{ref\ NN} = 1.501$ and $\delta_{ref\ NS} = 1.35$). The ^{1}H isotropic shielding were calculated with the GIAO method [35] using the optimized parameters obtained from B3LYP/6-311++G** method. The molecular orbital (MO) calculations such as the highest occupied MO (HOMO)–lowest unoccupied MO (LUMO) are also performed on the conformers of TNMH with the same level of DFT theory.

Results and discussion

Molecular conformation

On the basis of the conformer's standard definition, theoretically, TNMH has 25 different possible conformers. Based on functional groups, these conformers can be classified into three tautomeric classes: TI-I, T-A, and T-I, which have 15, 4, and 6 rotamers, respectively. Our theoretical calculations on TNMH show that TI-I conformers

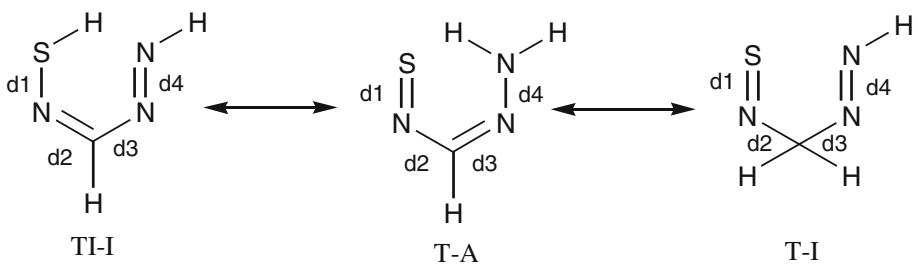

Fig. 1 Tautomery equilibrium in TNMH

are more stable than the other conformers. Comparison of all hydrogen- and non-hydrogen-bonded systems in TI-I, T-A, and T-I conformers using mean energies reveal the following order of energetic stability (the first and second values refer to calculations at 6-311++G** and aug-cc-pVTZ basis sets, respectively):

	TI-I	T-A	T-I
H-bonded: ΔE (kcal/mol)			
B3LYP	5.58, 5.15	4.53, 4.81	28.39, 28.73
MP2	5.57, 4.69	7.23, 3.63	25.21, 25.34
G2MP2	4.67	7.92	24.51
Non-hydrogen-bonded: ΔE (kcal/mol)			
B3LYP	3.94, 3.39	6.12, 6.76	28.46, 28.73
MP2	3.95, 3.44	9.76, 8.37	23.88, 24.55
G2MP2	3.51	9.52	24.49

From the above results, it can be concluded that the energy order in all of hydrogen-bonded systems are dependent of computational level. It was found out that the ZPVE correction could not considerably change the energy orders being an insensitive parameter.

In non-hydrogen-bonded systems, the TI-I conformers are more stable than T-A and T-I conformers. The extra stability of TI-I conformers is due to the existence of strong N–S, N=C, and N=N bonds and more π-electron delocalization in their frameworks. Theoretical calculations show that the T-A conformers are more stable than the T-I conformers. Although, in most amino compounds, the NH_2 functional group has the pyramidal shape, but it is noteworthy that the NH_2 functional group in all of T-A conformers is completely planar and lies in the molecular plane. This extra stability of T-A conformers is mainly due to the participation of nitrogen lone pair in the π-electron resonance; note because of the π-conjugation of double bonds in T-A skeleton.

TI-I group

Structural parameters and the relative energies computed with different methods are listed in Tables 1, 2, 3. All the different conformers of TI-I group are shown in Fig. 2.

The TI-I tautomers are quite interesting, since they show three types of intramolecular HBs, i.e., S–H···N (TI-I_2, TI-I_3, and TI-I_4), N–H···S (TI-I_5) and N–H···N (TI-I_9). The comparison of the relative energies of the different TI-I conformers shows that TI-I_6 is more stable conformer than all the other conformers (TI-I_1–TI-I_{15}). This stability is mainly due to the orientation of lone pairs of S and N atoms.

In the case of S–H···N hydrogen-bonding, it is accompanied by the lengthening of S–H bond and shortening of S···N distance and in the case of N–H···S and N–H···N bond, the lengthening of N–H bond and shortening of N···S and N···N distances would occur, respectively. The values of calculated geometrical parameters indicate stronger S–H···N interactions with respect to N–H···S and N–H···N bonds (see Tables 1, 2). Namely, H···N distance within S–H···N hydrogen-bond are regularly shorter than H···S bond. Furthermore, the comparison between the hydrogen-bond in TI-I_5 and TI-I_9 conformers showed that the N–H···N hydrogen-bond in TI-I_9 conformer was stronger than the N–H···S hydrogen-bond in TI-I_5 conformer. The values of H···N distance in TI-I_9 conformer and H···S distance in TI-I_5 conformer are about 2.177 and 2.563 Å, respectively, which supports the above results (see Tables 1, 2).

Regarding to the our theoretical results the hydrogen-bonding in TI-I_2 conformer is stronger than the others and this fact could be confirmed by comparison of the H···N distances in these conformers.

Geometrical parameters presented in (Tables 1, 2) showed that the N=N, N–C, N=C, and N–S bond distances in TI-I conformers were fairly similar and do not change noticeably even for the hydrogen-bonded conformers. This means that the energy function was insensitive to the changes of bond distance. In TI-I_2 conformer, the N=N, N=C, and S–H bond lengths are increased, whereas N–C and N–S bond lengths are decreased. These behaviors are caused by hydrogen-bond formation, which in fact increases the π-electrons resonance in the chelated ring.

T-A group

The structures of the different conformers of T-A group are shown in Fig. 3. The geometrical parameters and relative energies of T-A conformers are given in Tables 1, 2, 3. A comparison of the relative energies between different T-A conformers shows that T-A_3 is the most stable conformer.

The results of theoretical calculations on the stability orders of T-A conformer (Table 3) illustrate that in spite of the presence of N–H···S hydrogen-bonding in T-A_1 conformer; it is less stable than T-A_3 conformer. Here, theoretical calculation showed that the hydrogen-bond energies are not a major factor in determining the preferred conformations.

In the T-A_1 conformer, C=N, S=N, and N–H bond lengths have been risen, whereas N–N and C–N bond lengths are reducing. These behaviors are caused by hydrogen-bond formation, which in fact increases the π-electrons resonance in the chelated ring. Comparison of results presented in Tables 1, 4 reveals that, the N–H···S intramolecular HB energies theme in T-A_1 conformer was considerably stronger

Table 1 Geometrical parameters of TNMH conformers calculated at B3LYP/6-311++G** (bond lengths in Å, bond angles in °, energy in kcal/mol), whereby values in parentheses refer to calculations at the B3LYP/aug-cc-pVTZ level of theory

	NN	NC	NC	NS	S–H	N–H	S···H	N···H	N···S	N···N	SHN	NHS	NHN
TI-I_1	1.251 (1.247)	1.421 (1.418)	1.281 (1.277)	1.690 (1.678)	1.360 (1.356)	1.029 (1.027)	–	–	2.670 (2.676)	–	–	–	–
TI-I_2	1.254 (1.250)	1.418 (1.416)	1.283 (1.279)	1.668 (1.657)	1.359 (1.355)	1.030 (1.028)	–	2.059 (2.085)	3.027 (3.034)	–	123.3 (122.3)	–	–
TI-I_3	1.249 (1.245)	1.413 (1.411)	1.277 (1.273)	1.684 (1.673)	1.360 (1.357)	1.031 (1.028)	–	2.432 (2.453)	3.042 (3.046)	–	103.0 (102.3)	–	–
TI-I_4	1.243 (1.240)	1.416 (1.414)	1.274 (1.271)	1.681 (1.672)	1.360 (1.357)	1.049 (1.046)	–	2.424 (2.450)	3.049 (3.055)	–	103.7 (103.0)	–	–
TI-I_5	1.241 (1.238)	1.430 (1.427)	1.275 (1.272)	1.720 (1.705)	1.349 (1.346)	1.044 (1.040)	2.563 (2.506)	–	3.091 (3.063)	–	–	110.8 (112.8)	–
TI-I_6	1.247 (1.244)	1.416 (1.414)	1.275 (1.272)	1.709 (1.697)	1.349 (1.346)	1.031 (1.028)	–	–	2.917 (2.917)	–	–	–	–
TI-I_7	1.242 (1.238)	1.420 (1.418)	1.272 (1.269)	1.704 (1.693)	1.349 (1.346)	1.049 (1.046)	–	–	2.940 (2.938)	–	–	–	–
TI-I_8	1.242 (1.238)	1.425 (1.423)	1.271 (1.268)	1.714 (1.702)	1.348 (1.344)	1.032 (1.030)	–	–	–	–	–	–	–
TI-I_9	1.239 (1.236)	1.459 (1.457)	1.267 (1.264)	1.703 (1.691)	1.349 (1.345)	1.045 (1.043)	–	2.177 (2.178)	–	2.703 (2.702)	–	–	108.9 (108.9)
TI-I_{10}	1.249 (1.246)	1.416 (1.413)	1.274 (1.272)	1.703 (1.692)	1.348 (1.345)	1.030 (1.028)	–	–	–	–	–	–	–
TI-I_{11}	1.243 (1.240)	1.421 (1.418)	1.271 (1.268)	1.701 (1.690)	1.348 (1.345)	1.050 (1.047)	–	–	–	–	–	–	–
TI-I_{12}	1.242 (1.239)	1.424 (1.422)	1.27 (1.267)	1.688 (1.678)	1.366 (1.361)	1.032 (1.030)	–	–	–	–	–	–	–
TI-I_{13}	1.239 (1.236)	1.441 (1.437)	1.269 (1.266)	1.684 (1.676)	1.364 (1.360)	1.045 (1.042)	–	–	–	–	–	–	–
TI-I_{14}	1.250 (1.246)	1.414 (1.412)	1.273 (1.270)	1.678 (1.668)	1.366 (1.362)	1.030 (1.028)	–	–	–	–	–	–	–
TI-I_{15}	1.243 (1.240)	1.419 (1.416)	1.27 (1.267)	1.676 (1.667)	1.366 (1.362)	1.051 (1.047)	–	–	–	–	–	–	–
T-A_1	1.296 (1.292)	1.334 (1.331)	1.342 (1.338)	1.633 (1.626)	–	1.033 (1.031)	2.120 (2.113)	–	2.931 (2.924)	–	–	133.7 (134.0)	–
T-A_2	1.320 (1.320)	1.301 (1.297)	1.366 (1.364)	1.604 (1.596)	–	1.016 (1.005)	–	–	3.013 (3.005)	–	–	–	–
T-A_3	1.305 (1.302)	1.321 (1.317)	1.348 (1.346)	1.612 (1.605)	–	1.017 (1.014)	–	–	–	–	–	–	–
T-A_4	1.312 (1.309)	1.306 (1.302)	1.353 (1.350)	1.611 (1.604)	–	1.016 (1.003)	–	–	–	–	–	–	–
T-I_1	1.220 (1.215)	1.532 (1.531)	1.425 (1.421)	1.587 (1.581)	–	1.032 (1.030)	–	–	2.858 (2.849)	–	–	–	–
T-I_2	1.231 (1.228)	1.473 (1.469)	1.448 (1.444)	1.578 (1.572)	–	1.050 (1.047)	–	–	2.931 (2.923)	–	–	–	–
T-I_3	1.236 (1.233)	1.470 (1.467)	1.446 (1.442)	1.578 (1.573)	–	1.033 (1.031)	–	–	2.918 (2.913)	–	–	–	–
T-I_4	1.227 (1.224)	1.514 (1.507)	1.431 (1.429)	1.577 (1.570)	–	1.043 (1.040)	–	2.162 (2.170)	–	2.708 (2.714)	–	–	110.4 (110.4)
T-I_5	1.228 (1.224)	1.496 (1.493)	1.441 (1.438)	1.577 (1.571)	–	1.049 (1.046)	–	–	–	–	–	–	–
T-I_6	1.236 (1.232)	1.476 (1.473)	1.453 (1.450)	1.574 (1.568)	–	1.033 (1.030)	–	–	–	–	–	–	–

than that in TI-I_5 conformer. Furthermore, the greater value of S···N distance in TI-I_5 against the T-A_1 confirms the existence of weaker hydrogen-bonding in TI-I_5 conformer. Analysis of the geometrical parameters showed that the N–H···S bond angle in the T-A_1 is closer to 180° and therefore, the strength of the hydrogen-bond in T-A_1 is greater than in TI-I_5.

The ^{1}H chemical shifts for all hydrogen-bonded systems in all conformers calculated by the GIAO method at the B3LYP/6-311++G** level are collected in Table 4. The results of this table confirm that the strengthening of hydrogen-bond causes ^{1}H chemical shift of H moves to down fields.

The effect of π-electron delocalization on the characteristic of RAHB has been also investigated [36, 37]. The consequence of the π-electron delocalization within RAHBs are as follows: (I) the shortening of S···N distance; (II) the strengthening of H-bond; (III) the shift of the proton toward the center of S···N contact; (IV) the equalization of C–N, C=N bonds; and (V) the equalization of N–N and S=N bonds. The equalization of the corresponding bonds for RAHB system (points (IV) and (V)) is the direct geometrical consequence of the π-electron delocalization. The parameter of such delocalization has been proposed:

$$Q = (d_2 - d_3) + (d_4 - d_1)$$

where d_1, d_2, d_3, and d_4 are bond lengths (Fig. 1).

The correlations of Q with the other parameters of the hydrogen-bond have been investigated showing that the lowest the value of Q the stronger is the H-bond and the greater is the π-electron delocalization. The values of Q-parameters for the system investigated here are given in Table 4. As it is obvious from this table, the greatest value of Q has occurred for TI-I_9 and the lowest value of Q was for T-A_1. Comparison of Q in TI-I_2, TI-I_3, and TI-I_4 conformers shows that Q value in TI-I_2 is lower than TI-I_3 and TI-I_4. This fact confirms that the resonance in this conformer is more pronounced than the TI-I_3 and TI-I_4.

In the present study, the use of topological electron density properties in the ring critical points of the aromatic systems has been investigated as a way of quantifying aromaticity indicators. Table 4 lists all values obtained from the different aromaticity criteria. The results obtained show among aromaticity indices, the HOMA, PDI, FLU indicators correctly predict the most aromatic species, whereas we have found that NICS (1.5) index seems to be supported fairly. Therefore, it is evident that with strengthening the intramolecular HB, in T-A_1, aromaticity indices HOMA and PDI increase and FLU index decrease (Table 4). This fact confirms that the resonance in this conformer is more pronounced than the other conformers.

The results corresponding to the transition state between T-A_1 and TI-I_2 structures (TS 2/1) listed in Table 5. In general, the reaction path could be defined as the curve on the potential energy surface connecting the reactants and products through the transition state (see Fig. 4). The free-energy barrier for proton transfer is 5.08 kcal/mol.

T-I group

The structurally possible T-I tautomeric conformers are shown in Fig. 5, mentioning that the geometrical parameters and relative energies can be observed in Tables 1, 2, 3.

The T-I_1 conformer is more stable than the other T-I conformers in all of computational levels. This stability may be mainly due to the orientation of lone pairs of sulfur and nitrogen atoms and arises from interactions formed between other functional groups within the rotamers. The values of ρ_{BCP} and $\nabla^2_{\rho_{BCP}}$, at this BCP, are about 0.01948 and 0.05902 au, respectively, which suggest the presence of a relatively strong interaction. Because T-I_1 has the maximum repulsion interaction, we carried out a detail analysis by AIM theory. The obtained results clearly show an additional BCP between two nitrogen (N) and sulfur (S) atoms.

Among the T-I conformers, there is one conformer (T-I_4) that contain N···H–N bond. The strength of intramolecular hydrogen-bonding in this conformer calculated at about −5.22 kcal/mol.

Another index closely related with the relative strength of HB is the shifting of the S–H (TI-I_2, TI-I_3, and TI-I_4) and N–H (TI-I_5, TI-I_9, T-A_1, and T-I_4) stretching frequencies. It is well-established that the stronger the HB, the larger is this shifting. To estimate this effect, we need a reference system where the HB is absent and which presents an electronic structure similar to that of the hydrogen-bonded species. For example for TI-I_2, T-A_1, and T-I_4, the most suitable candidates are rotamer of TI-I_{10}, T-A_4, and T-I_6. Our calculations (see Table 4) indicate that the S–H stretching frequency for the TI-I_2 conformer appears red-shifted by ca. 96.59 cm^{-1} with respect to that in TI-I_{10} and the N–H stretching frequency for the T-A_1 and T-I_4 tautomer appears red-shifted by ca. 359.37 and 140.50 cm^{-1} with respect to that in T-A_4 and T-I_6, respectively. Comparison of results presented in Table 4 reveals that, the intramolecular HB energies in T-A conformers were stronger than TI-I and T-I conformers.

AIM analysis

The formation of HB is associated with the appearance of a bond critical point between the hydrogen atom of donor group and acceptor atom. Poplier [27] proposed a set of criteria for the specification of hydrogen-bonding within the AIM formalism. In order to have a deeper knowledge of the nature of the possible hydrogen-bonds in TNMH conformers, a topological analysis of electronic charge density, ρ_{BCP},

Table 2 Geometrical parameters of TNMH conformers calculated at MP2/6-311++G** (bond lengths in Å, bond angles in °, energy in kcal/mol), whereby values in parentheses refer to calculations at the MP2/aug-cc-pVTZ level of theory

	NN	NC	NC	NS	S–H	N–H	S···H	N···H	N···S	N···N	SHN	NHS	NHN
TI-I_1	1.270 (1.268)	1.425 (1.415)	1.292 (1.290)	1.686 (1.677)	1.342 (1.346)	1.030 (1.028)	–	–	2.658 (2.600)	–	–	–	–
TI-I_2	1.271 (1.269)	1.423 (1.415)	1.293 (1.291)	1.670 (1.661)	1.342 (1.346)	1.031 (1.028)	–	2.059 (2.013)	3.027 (2.992)	–	124.5 (124.8)	–	–
TI-I_3	1.266 (1.263)	1.422 (1.417)	1.286 (1.282)	1.687 (1.682)	1.344 (1.346)	1.031 (1.028)	–	2.365 (2.353)	3.016 (3.004)	–	105.5 (105.3)	–	–
TI-I_4	1.259 (1.257)	1.425 (1.420)	1.283 (1.279)	1.684 (1.681)	1.344 (1.347)	1.048 (1.046)	–	2.360 (2.345)	3.024 (3.011)	–	106.2 (106.1)	–	–
TI-I_5	1.260 (1.257)	1.438 (1.431)	1.282 (1.280)	1.724 (1.718)	1.333 (1.336)	1.043 (1.041)	3.171 (2.773)	–	3.277 (3.075)	–	–	86.5 (96.8)	–
TI-I_6	1.265 (1.262)	1.423 (1.418)	1.284 (1.281)	1.708 (1.704)	1.335 (1.337)	1.031 (1.028)	–	–	2.881 (2.860)	–	–	–	–
TI-I_7	1.259 (1.256)	1.427 (1.422)	1.282 (1.279)	1.704 (1.700)	1.335 (1.337)	1.049 (1.045)	–	–	2.904 (2.881)	–	–	–	–
TI-I_8	1.242 (1.257)	1.425 (1.427)	1.271 (1.278)	1.714 (1.707)	1.348 (1.335)	1.032 (1.029)	–	–	–	–	–	–	–
TI-I_9	1.256 (1.252)	1.464 (1.459)	1.277 (1.274)	1.701 (1.696)	1.334 (1.336)	1.045 (1.044)	–	2.113 (2.093)	–	2.681 (2.665)	–	–	111.7 (112.0)
TI-I_{10}	1.267 (1.264)	1.420 (1.415)	1.284 (1.281)	1.705 (1.699)	1.334 (1.336)	1.030 (1.028)	–	–	–	–	–	–	–
TI-I_{11}	1.26 (1.257)	1.426 (1.420)	1.281 (1.278)	1.703 (1.698)	1.334 (1.336)	1.049 (1.046)	–	–	–	–	–	–	–
TI-I12	1.261 (1.258)	1.431 (1.427)	1.279 (1.275)	1.693 (1.688)	1.349 (1.350)	1.032 (1.029)	–	–	–	–	–	–	–
TI-I_{13}	1.257 (1.253)	1.445 (1.441)	1.279 (1.275)	1.688 (1.683)	1.348 (1.350)	1.045 (1.043)	–	–	–	–	–	–	–
TI-I_{14}	1.268 (1.264)	1.420 (1.415)	1.282 (1.279)	1.684 (1.679)	1.349 (1.351)	1.030 (1.027)	–	–	–	–	–	–	–
TI-I_{15}	1.260 (1.257)	1.425 (1.419)	1.279 (1.276)	1.682 (1.678)	1.350 (1.351)	1.049 (1.046)	–	–	–	–	–	–	–
T-A_1	1.314 (1.306)	1.336 (1.335)	1.353 (1.344)	1.629 (1.631)	–	1.035 (1.035)	2.038 (2.013)	–	2.871 (2.851)	–	–	135.7 (136.2)	–
T-A_2	1.320 (1.347)	1.301 (1.297)	1.366 (1.383)	1.604 (1.603)	–	1.016 (1.007)	–	–	–	–	–	–	–
T-A_3	1.305 (1.310)	1.321 (1.322)	1.348 (1.354)	1.612 (1.611)	–	1.017 (1.014)	–	–	–	–	–	–	–
T-A_4	1.344 (1.332)	1.303 (1.303)	1.376 (1.365)	1.604 (1.607)	–	1.018 (1.005)	–	–	–	–	–	–	–
T-I_1	1.244 (1.227)	1.525 (1.568)	1.43 (1.404)	1.605 (1.621)	–	1.031 (1.028)	–	–	2.738 (2.475)	–	–	–	–
T-I_2	1.251 (1.248)	1.469 (1.463)	1.465 (1.458)	1.588 (1.587)	–	1.047 (1.045)	–	–	2.867 (2.845)	–	–	–	–
T-I_3	1.257 (1.254)	1.466 (1.462)	1.462 (1.455)	1.587 (1.587)	–	1.032 (1.030)	–	–	2.861 (2.843)	–	–	–	–
T-I_4	1.252 (1.248)	1.485 (1.480)	1.454 (1.451)	1.583 (1.581)	–	1.042 (1.040)	–	2.054 (2.051)	–	2.675 (2.670)	–	–	115.7 (115.6)
T-I_5	1.250 (1.246)	1.479 (1.475)	1.456 (1.453)	1.585 (1.584)	–	1.048 (1.044)	–	–	–	–	–	–	–
T-I_6	1.256 (1.253)	1.463 (1.467)	1.474 (1.458)	1.584 (1.582)	–	1.032 (1.029)	–	–	–	–	–	–	–

Table 3 Stability order (SO) and relative energies (RE) TI-I, T-A, and T-I conformers at various computational methods (kcal/mol) in gas phase

B3LYP		B3LYP*		MP2		MP2*		G2MP2	
SO	RE	SO	RE	SO	RE	SO	RE	SO	RE
$TI\text{-}I_6$	0.00	$TI\text{-}I_6$	0.00	$TI\text{-}I_6$	0.00	$TI\text{-}I_6$	0.00	$TI\text{-}I_6$	0.00
$TI\text{-}I_{10}$	0.42	$TI\text{-}I_{10}$	0.26	$TI\text{-}I_{10}$	0.27	$TI\text{-}I_{10}$	0.35	$TI\text{-}I_{10}$	0.58
$TI\text{-}I_3$	0.67	$TI\text{-}I_3$	0.56	$TI\text{-}I_3$	0.95	$TI\text{-}I_3$	0.63	$TI\text{-}I_2$	0.75
$TI\text{-}I_{14}$	1.25	$TI\text{-}I_{14}$	0.72	$TI\text{-}I_{14}$	1.19	$TI\text{-}I_{14}$	0.99	$TI\text{-}I_3$	0.76
$T\text{-}A_3$	1.97	$TI\text{-}I_1$	2.61	$TI\text{-}I_1$	2.41	$TI\text{-}I_1$	1.62	$TI\text{-}I_{14}$	1.17
$TI\text{-}I_1$	2.47	$T\text{-}A_3$	3.03	$TI\text{-}I_8$	4.88	$T\text{-}A_1$	3.63	$TI\text{-}I_1$	2.15
$T\text{-}A_1$	4.53	$TI\text{-}I_7$	4.06	$TI\text{-}I_7$	5.19	$T\text{-}A_3$	4.33	$TI\text{-}I_7$	4.29
$TI\text{-}I_8$	4.79	$TI\text{-}I_4$	4.21	$TI\text{-}I_{12}$	5.20	$TI\text{-}I_7$	4.39	$TI\text{-}I_8$	4.45
$TI\text{-}I_7$	4.80	$TI\text{-}I_8$	4.62	$TI\text{-}I_4$	5.57	$TI\text{-}I_8$	4.43	$TI\text{-}I_4$	4.62
$TI\text{-}I_4$	4.96	$T\text{-}A_1$	4.81	$TI\text{-}I_2$	5.58	$TI\text{-}I_4$	4.54	$TI\text{-}I_9$	4.92
$TI\text{-}I_2$	5.16	$TI\text{-}I_{11}$	4.90	$TI\text{-}I_9$	5.99	$TI\text{-}I_2$	4.82	$TI\text{-}I_{12}$	5.24
$T\text{-}A_4$	5.28	$TI\text{-}I_{12}$	5.19	$T\text{-}A_3$	6.04	$TI\text{-}I_{12}$	5.23	$TI\text{-}I_{11}$	5.39
$TI\text{-}I_{12}$	5.73	$TI\text{-}I_2$	5.21	$TI\text{-}I_{11}$	6.36	$TI\text{-}I_9$	5.28	$TI\text{-}I_{13}$	5.66
$TI\text{-}I_{11}$	5.98	$T\text{-}A_4$	5.53	$TI\text{-}I_{13}$	6.46	$TI\text{-}I_{11}$	5.39	$T\text{-}A_3$	6.02
$TI\text{-}I_9$	6.16	$TI\text{-}I_{15}$	5.55	$T\text{-}A_1$	7.22	$TI\text{-}I_{13}$	5.72	$TI\text{-}I_{15}$	6.13
$TI\text{-}I_{13}$	6.89	$TI\text{-}I_9$	5.78	$TI\text{-}I_{15}$	7.52	$TI\text{-}I_{15}$	6.23	$T\text{-}A_1$	7.92
$TI\text{-}I_{15}$	7.05	$TI\text{-}I_{13}$	6.05	$T\text{-}A_4$	9.27	$T\text{-}A_4$	8.04	$TI\text{-}I_5$	8.39
$TI\text{-}I_5$	10.94	$TI\text{-}I_5$	9.92	$TI\text{-}I_5$	9.75	$TI\text{-}I_5$	8.20	$T\text{-}A_4$	9.26
$T\text{-}A_2$	11.12	$T\text{-}A_2$	11.71	$T\text{-}A_2$	13.98	$T\text{-}A_2$	12.73	$T\text{-}A_2$	13.28
$T\text{-}I_1$	26.19	$T\text{-}I_1$	26.92	$T\text{-}I_1$	20.63	$T\text{-}I_1$	21.22	$T\text{-}I_4$	22.22
$T\text{-}I_3$	26.28	$T\text{-}I_4$	26.92	$T\text{-}I_4$	21.72	$T\text{-}I_4$	22.79	$T\text{-}I_8$	22.58
$T\text{-}I_6$	26.77	$T\text{-}I_8$	27.26	$T\text{-}I_8$	21.98	$T\text{-}I_8$	23.38	$T\text{-}I_1$	23.68
$T\text{-}I_4$	28.39	$T\text{-}I_6$	28.73	$T\text{-}I_6$	25.21	$T\text{-}I_6$	25.34	$T\text{-}I_6$	24.51
$T\text{-}I_5$	31.10	$T\text{-}I_7$	30.73	$T\text{-}I_7$	27.47	$T\text{-}I_7$	27.60	$T\text{-}I_7$	26.82
$T\text{-}I_2$	31.98	$T\text{-}I_3$	31.82	$T\text{-}I_3$	27.62	$T\text{-}I_3$	27.75	$T\text{-}I_3$	27.14

Sign* refer to calculations at the aug-cc-pVTZ basis set

and its Laplacian ($\nabla^2_{\rho_{BCP}}$) were performed. It is well-known that the hydrogen-bonded energy is related to (ρ) at the H···Y BCP and (∇^2_ρ), of electron density at BCP of two hydrogen-bonded atoms [36]. The topological parameters in all of the hydrogen-bonded forms ($TI\text{-}I_2$, $TI\text{-}I_3$, $TI\text{-}I_4$, $TI\text{-}I_5$, $TI\text{-}I_9$, $T\text{-}A_1$, and $T\text{-}I_4$) at the B3LYP/6-311++G** level of theory are evaluated and the results are collected in Table 6. These characteristics of electron densities and its Laplacian at BCPs signify the presence of a HB interaction. The property of the Laplacian of the electron density, which is used to determine regions of concentration and depletion of the electron charge density, forms a basis for the classification of the atomic interactions. The atomic interactions were classified into two general classes, shared interactions ($\nabla^2_\rho < 0$) and closed-shell interactions ($\nabla^2_\rho > 0$).

The calculated electron density properties of selected conformers showed that N···H and S···H bodings have low ρ_{BCP} (the range of 0.02765 and 0.014199 for $TI\text{-}I_2$, $TI\text{-}I_3$, $TI\text{-}I_4$, $TI\text{-}I_9$, and $T\text{-}I_4$ conformers and about 0.037681 and 0.013325 for $T\text{-}A_1$ and $TI\text{-}I_5$ conformers, respectively) and positive $\nabla^2_{\rho_{BCP}}$ values. These properties are typical for closed-shell interaction for them.

Comparison between the electron densities of $TI\text{-}I_2$, $TI\text{-}I_3$, $TI\text{-}I_4$, $TI\text{-}I_9$, and $T\text{-}I_4$ for the N···H bondings (and $TI\text{-}I_5$, $T\text{-}A_1$ for the H···S bondings) showed that ρ_{BCP} for the $T\text{-}A_1$ conformer are higher than the corresponding value for $TI\text{-}I_5$ conformer, and the values of $TI\text{-}I_2$ is higher than those of $TI\text{-}I_3$, $TI\text{-}I_4$ and $TI\text{-}I_9$ conformers, and the values of $T\text{-}I_4$ is higher than those of $TI\text{-}I_9$ conformer. As a consequence, the strength of hydrogen-bond in $T\text{-}A_1$, $TI\text{-}I_2$, and $T\text{-}I_4$ are greater than the $TI\text{-}I_5$, $TI\text{-}I_3$, $TI\text{-}I_4$, and $TI\text{-}I_9$, respectively. These results are in line with the hydrogen-bond energies which are calculated by Espinosa method (see Table 4).

NBO analysis

The results of our NBO analysis (occupation number for the assignments and their orbital energies) for TNMH conformers are provided in Table 7. In this table, the NBO occupation numbers for $\sigma^*_{(S-H)}$, $\sigma^*_{(N-H)}$ antibonds, the sulfur and nitrogen lone

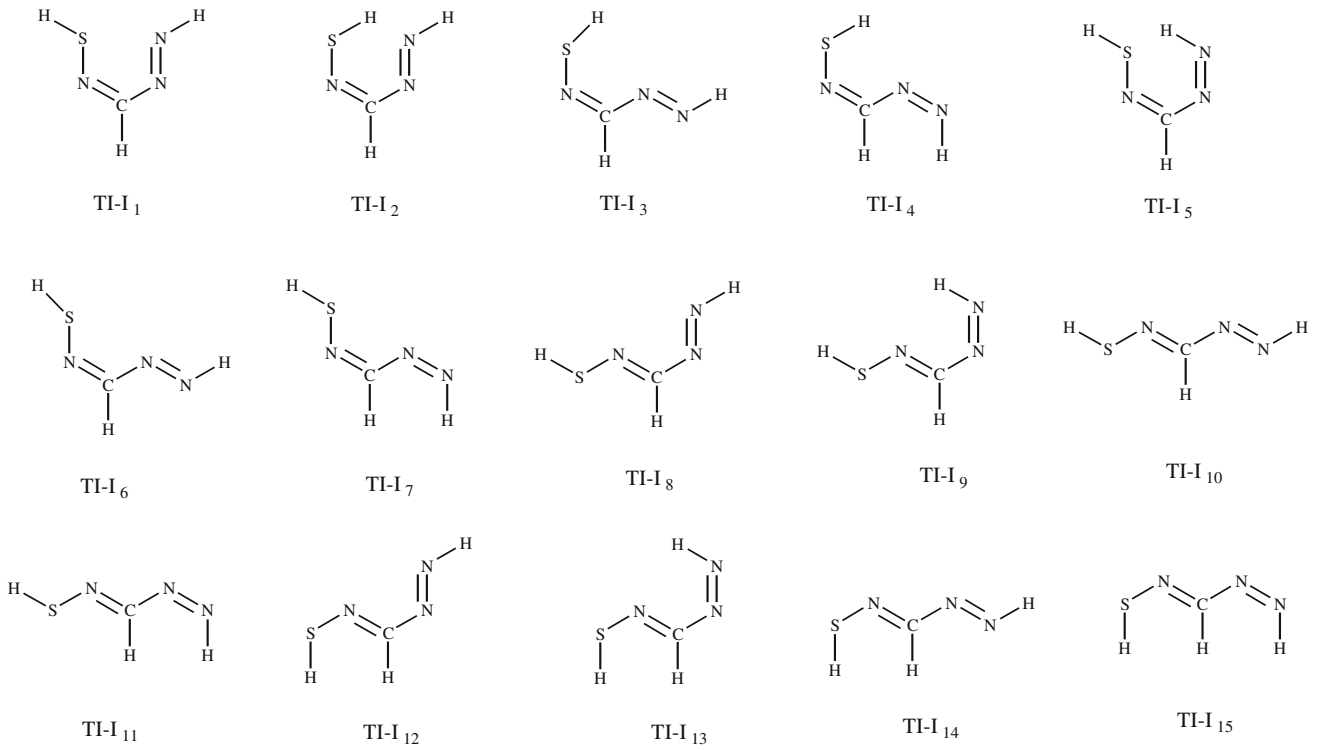

Fig. 2 Possible conformers in TI-I

Fig. 3 Possible conformers in T-A

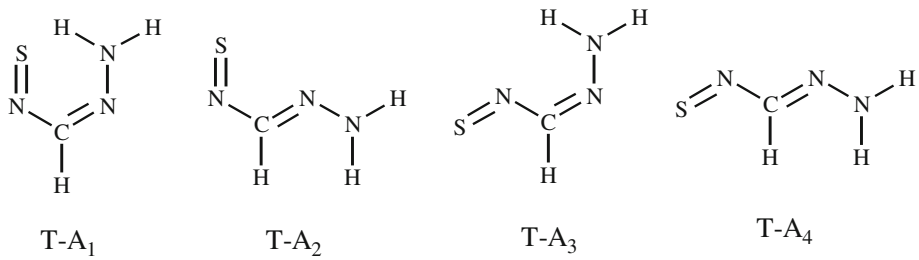

pairs electrons (nS and nN, respectively), and their respective orbital energies, *E*, are shown. Furthermore, the donor–acceptor interaction and their second-order perturbation stabilization energies $E^{(2)}$ (calculated at B3LYP/6-311++G** level of theory) for the chelated rings of TI-I_2, TI-I_3, TI-I_4, TI-I_5, TI-I_9, T-A_1, and T-I_4 are presented in Table 7. In the NBO analysis of the hydrogen-bonded systems, the charge transfer between the lone pair's electrons of the proton acceptor and antibonds of proton donors is the most important interaction. The results of NBO analysis showed that in the chelated structures of the TNMH conformers, two lone pairs electrons of sulfur (or nitrogen) atoms participate as donor and $\sigma^*_{(S-H)}$ or $\sigma^*_{(N-H)}$ antibonds as acceptors. The NBO results again support the order of intramolecular hydrogen-bonding strength in TNMH conformers.

Figure 6 displays the two-dimensional contour plots of the interaction between the electron lone pairs of sulfur and nitrogen (nS and nN, respectively) with antibonding N–H or S–H orbitals in T-A_1 and TI-I_2 conformers, respectively.

HOMO–LUMO analysis

The HOMO and LUMO are the main orbital, which take part in chemical stability [38]. The HOMO represents the stability to donate an electron, LUMO as an electron acceptor represents the ability to obtain an electron. This electron transition absorption corresponds to the transition from the ground to the first excited state and is mainly described by an electron excitation from the HOMO to the LUMO. The energy gap between the HOMOs and the LUMOs, is a critical parameter in determining molecular electrical transport properties because it is a measure of electron conductivity. The plots of HOMOs and LUMOs are shown in Fig. 7. The energy values of HOMO are computed −5.88 and −6.81 eV and LUMO are −3.79 and −3.15 eV, and the energy gap values are 2.09 and 3.66 eV in T-A_1 and TI-I_2 conformers, respectively. Consequently, the lower in the HOMO and LUMO energy gap in T-A_1

Table 4 The energies of the intramolecular hydrogen-bond (E^*_{HB}) and RBMs (E_{BR}, in kcal/mol), aromaticity indices, stretching frequencies (in cm^{-1}), the topological parameters (in au) and values of dipole moment (in *D*) in the chelated ring of TNMH conformers (values in parentheses refer to calculations in water solution and in brackets refer to calculations in CCl_4 solution)

	TI-I_2	TI-I_3	TI-I_4	TI-I_5	TI-I_9	T-A_1	T-I_4
E^*_{HB}	−6.85	−2.84	−2.86	−2.51	−5.07	−9.50	−5.22
	(−5.98)	(−2.65)	–	–	(−4.91)	(−8.35)	(−4.89)
	[−6.65]	[−2.73]	[−2.66]	–	–	[−9.07]	[−5.14]
E_{BR}	20.82	14.78	15.64	53.51	49.34	28.82	63.99
HOMA	0.666	0.609	0.588	0.340	0.260	0.991	–
PDI	0.05819	0.06195	0.06169	0.05425	0.06171	0.08977	0.05015
ATI	1.13533	1.12866	1.13005	1.10871	1.10639	1.08276	1.13085
FLU	0.05292	0.07081	0.0692	0.05826	0.06461	0.01899	0.18772
NICS (1.5)	−1.4966	−1.0705	−0.976	−2.3324	−2.7340	−1.9610	−1.1551
Q	0.54912	0.5717	0.58035	0.63445	0.65625	0.32939	0.43368
δ (ppm)	11.4592	8.6142	9.3791	14.9158	16.1708	20.4269	22.2579
$\rho(r_c)$	0.01322	0.01397	0.01400	0.01179	0.02041	0.01490	0.02018
$\nabla^2_\rho(r_c)$	0.06855	0.06172	0.06219	0.05435	0.11517	0.08638	0.12055
$G(r_c)$	0.02182	0.01092	0.011	0.00956	0.01867	0.02401	0.01868
$H(r_c)$	2.1E−05	0.00187	0.0019	0.00155	0.00254	−0.0062	0.00206
$\mu(D)$	1.97	2.28	1.05	2.29	3.66	3.71	2.52
	(3.10)	(3.56)	(1.92)	(3.20)	(4.49)	(5.91)	(3.58)
	[2.38]	[2.72]	[1.33]	[2.52]	[4.23]	[4.50]	[2.97]
$\Delta\upsilon$	96.59	92.13	84.50	208.77	206.88	359.37	140.50

Table 5 Geometrical parameters (bond lengths in Å, bond angles in °), and values of dipole moment (in *D*) 0f calculated at B3LYP/6-311++G** level of theory

	TI-I_2	TS 2/1	T-A_1
H–N	2.059	1.356	1.033
NN	1.254	1.271	1.296
NC	1.418	1.383	1.334
CN	1.283	1.304	1.342
NS	1.668	1.672	1.633
S–H	1.359	1.546	2.120
H–N–N	114.8	114.4	121.2
N–N–C	116.3	116.7	120.4
N–C–N	132.8	130.7	132.3
C–N–S	130.3	123.3	125.1
N–S–H	102.4	90.8	87.3
S–H–N	123.3	144.1	133.7
$\mu(D)$	1.97	2.89	3.71

explains the eventual charge transfer interactions taking place within the molecule. The frontier orbitals were drawn to understand the bonding scheme of present compounds. The positive phase is red and the negative one is green. According to Fig. 7, the HOMO of T-A_1 conformer shows bonding character at N–H···S. The LUMO has a larger electronic projection over S in this conformer. The HOMO of TI-I_2 conformer shows antibonding character at S–H···N. For the LUMO of TI-I_2 conformer, the electronic projection decreases over S compared to LUMO of T-A_1 conformer.

Rotation barriers method (RBM)

Barrier energy to internal rotation about the single bond is one of the major factors controlling the conformations of molecules [39]. The method here proposed (labeled in the following as RBM) refers exclusively to the intramolecular HB. Such barriers were first recognized in the study of ethane to reconcile experimental heat capacity measurements and statistical mechanics calculation at low temperature [40, 41]. A method for evaluating the energy of intramolecular hydrogen bridges utilizing the rotation barriers of the donor and/or of the acceptor groups is proposed. The procedure has been tested successfully on various molecules containing S–H···N, N–H···S, and N–H···N bridges. The rotational barriers (E_{BR}) around N–H (T-A_1, TI-I_5, TI-I_9, and T-I_4) and S–H (TI-I_2, TI-I_3 and TI-I_4) bonds were investigated by DFT calculations using 6-311++G** basis set in gas phase. The barriers are in the ranges of 14.78–63.99 kcal/mol (see Table 4).

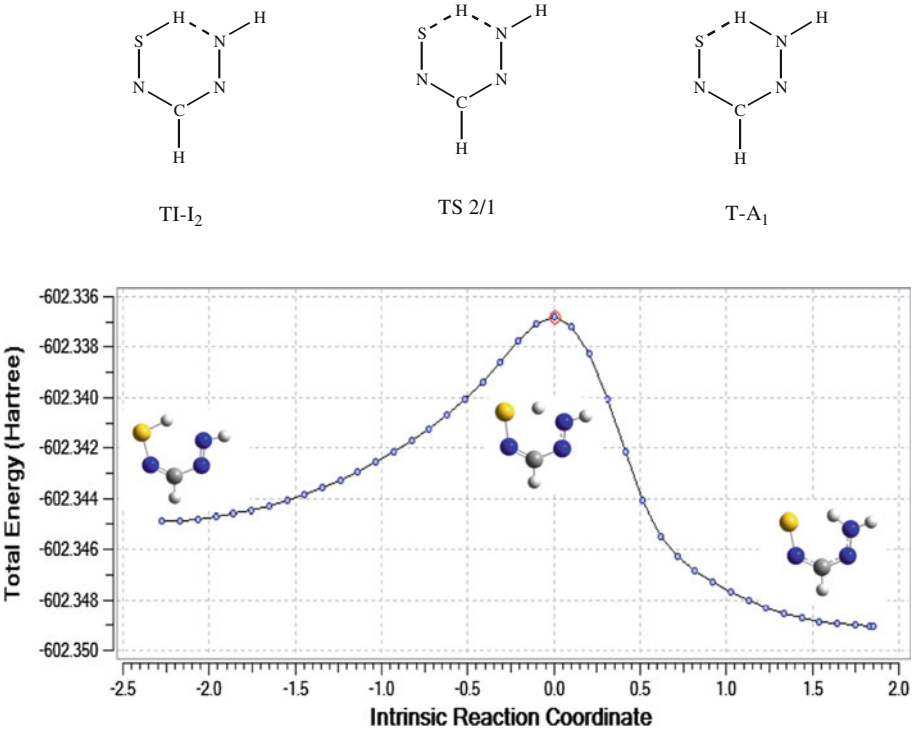

Fig. 4 B3LYP/6-311++G** calculated total energy values versus IRCs for compound TI-I_2

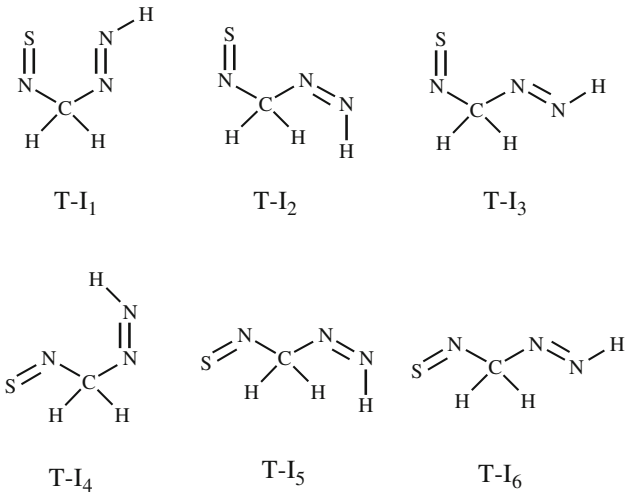

Fig. 5 Possible conformers in T-I

The conformers in water and CCl_4 solutions

In order to investigate the geometry and the intramolecular HB energy changes in the various TNMH conformers, B3LYP- and MP2/6-311++G** optimization in water and CCl_4 solutions were carried out. The solvent effect was calculated using the PCM model. It is known that the hydrogen-bond strength in solution is weaker when compared to the gas phase and its energy decreases when the dipole moment of the solvent increases. The topological and geometrical parameters of TI-I, T-A, and T-I conformer in water and CCl_4 solutions have been presented in Tables 6, 8. The stability orders of TI-I, T-A, and T-I conformers are given in Table 9. After optimization TI-I_5 convert to TI-I_7. Comparison of all hydrogen-bonded and non-hydrogen-bonded systems in TI-I, T-A, and T-I conformers using mean energies revealed the following order of energetic stability (in water and CCl_4 solutions): (The first and second values in parentheses and brackets refer to calculations at B3LYP- and MP2/6-311++G** levels of theory, respectively).

	TI-I	T-A	T-I
H-bonded: ΔE (kcal/mol)			
Water	(5.42, 2.44)	(6.31, 9.42)	(31.72, 27.85)
CCl_4	[4.61, 4.93]	[4.99, 7.92]	[29.43, 26.04]
Non-H-bonded: ΔE (kcal/mol)			
Water	(3.33, 3.38)	(3.12, 9.30)	(29.86, 23.84)
CCl_4	[3.52, 3.62]	[4.89, 9.04]	[28.91, 24.37]

Intramolecular HB energies of the TI-I, T-A, and T-I conformers have been calculated using the Espinosa and Molins method [22] and presented in Table 4. Probe of these values depicted that hydrogen-bonding strength of TI-I_2, TI-I_3, TI-I_4, TI-I_9, T-A_1, and T-I_4 conformers in gas phase is stronger than that of water and CCl_4 solutions. The comparison of N···H and S···H distances in all of the conformers in gas phase and in water and CCl_4 solutions showed that the hydrogen-bonding strength in gas phase is stronger than that of water and CCl_4 solutions. For example, the hydrogen-bond energy for the N–H···S bridge in

Table 6 The topological parameters (in au) of chelated ring—the electron densities at H···X BCPs, for TI-I, T-A, and T-I conformers (values in parenthesis refer to calculations in water solution and values in brackets refer to CCl_4 solution)

Conformer	X	ρ(X···H)	∇^2_ρ(X···H)
TI-I_2	N	0.027650 (0.025110) [0.027080]	0.087350 (0.080270) [0.085830]
TI-I_3	N	0.014199 (0.013458) [0.013757]	0.051175 (0.048791) [0.049946]
TI-I_4	N	0.014234 (…) […]	0.051588 (0.013376) [0.049791]
TI-I_5	S	0.013325 (…) […]	0.044432 (…) […]
TI-I_9	N	0.020850 (…) [0.020330]	0.084830 (…) [0.083210]
T-A_1	S	0.037681 (0.034363) [0.068793]	0.071104 (0.036451) [0.070475]
T-I_4	N	0.021718 (0.020804) [0.021503]	0.082958 (0.078426) [0.081711]

Table 7 NBO analysis of the chelated ring of TNMH conformers

Conformers	TI-I_2	TI-I_3	TI-I_4	TI-I_5	TI-I_9	T-A_1	T-I_4
LP → σ^*_{NH}	–	–	–	–	9.14	24.71	2.00
LP → σ^*_{SH}	6.60	0.81	0.91	–	–	–	–
O.N.$_{(LP)}$	1.96296	1.95001	1.91890	1.86857	1.93943	1.89331	1.93532
$\varepsilon_{(LP)}$	−0.50534	−0.45486	−0.43696	−0.28835	−0.42714	−0.27985	−0.46367
O.N.$_{(S–H)}$	0.04951	0.03164	0.03001	–	–	–	–
$\varepsilon_{(S–H)}$	0.16642	0.15298	0.14959	–	–	–	–
O.N.$_{(N–H)}$	–	–	–	0.03742	0.04292	0.10489	0.04320
$\varepsilon_{(N–H)}$	–	–	–	0.33381	0.35817	0.33786	0.35703

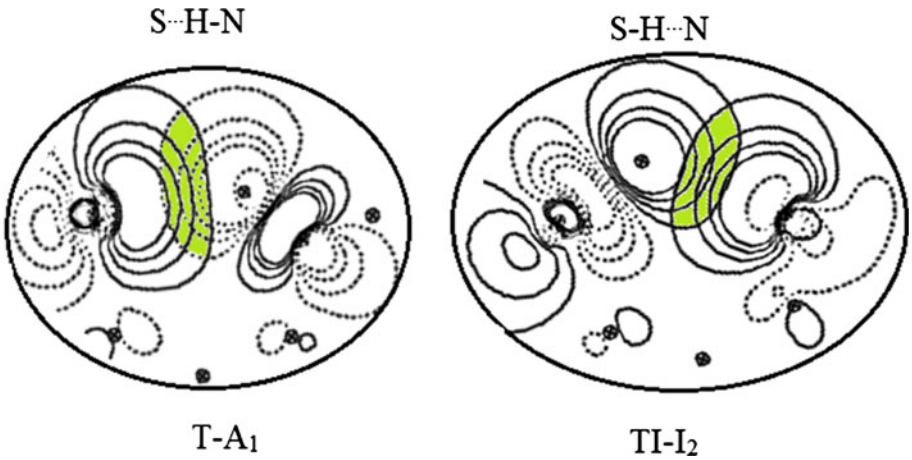

Fig. 6 Contour *diagram* showing the orbital (NBOs) interactions (LPY-$\sigma^*_{(X–H)}$ hyperconjugative charge transfer interaction in X–H···Y hydrogen-bond) involved information of the S···H–N or S–H···N Intramolecular hydrogen-bond in the T-A_1 and TI-I_2 of TNMH

T-A_1 conformer reduces to −8.35 kcal/mol in water solution (in gas phase and CCl_4 solution are −9.50 and −9.07 kcal/mol, respectively), whereas E_{HB} for S–H···N bridge in TI-I_2 conformer in gas phase is −6.85 kcal/mol, which is close to CCl_4 solution (−6.65 kcal/mol) and decreases to −5.98 kcal/mol in water solution.

The dipole moment have been calculated with B3LYP/6-311++G** level. Dipole moment reflects the molecular charge distribution and is given as a vector in three dimensions. Therefore, it can be used as descriptor to depict the charge movement across the molecule. Direction of the dipole moment vector in a molecule depends on the centers of positive and negative charges. Dipole moments are strictly determined for neutral molecules. For charged systems, its value depends on the choice of origin and molecular orientation. As a result of DFT (B3LYP) calculations the highest dipole moment was observed for compounds in water solution, whereas the smallest one was observed for compounds in gas phase (Table 4).

Conclusions

A theoretical study of 25 possible conformers of (TNMH), has been carried out by means of ab initio (MP2/aug-

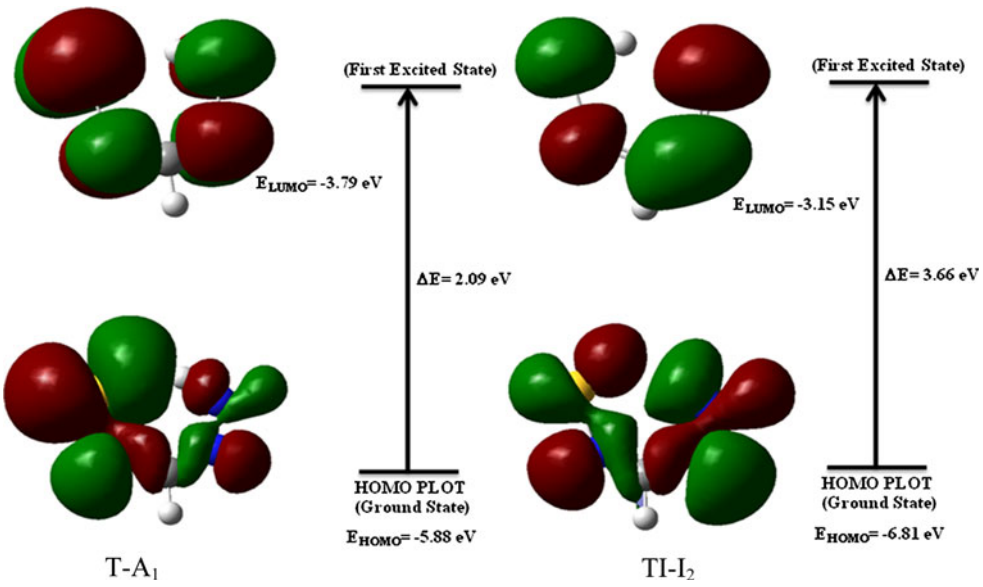

Fig. 7 HOMO and LUMO of T-A_1 and TI-I_2 conformers as obtained with B3LYP/6-311++G** level of theory

Table 8 Geometrical parameters of the TI-I, T-A, and T-I conformers calculated at the B3LYP/6-311++G** level of theory in water solution (values in parenthesis refer to calculations in carbon tetrachloride solution)

	NN	NC	NC	NS	S–H	N–H	N···H	S···H	N···S	N···N
TI-I_1	1.251 (1.251)	1.424 (1.422)	1.282 (1.281)	1.696 (1.692)	1.377 (1.365)	1.042 (1.033)	–	–	2.707 (2.682)	–
TI-I_2	1.252 (1.253)	1.424 (1.420)	1.282 (1.283)	1.676 (1.671)	1.362 (1.359)	1.042 (1.034)	2.113 (2.071)	–	3.041 (3.030)	–
TI-I_3	1.248 (1.249)	1.416 (1.414)	1.278 (1.277)	1.693 (1.687)	1.380 (1.366)	1.042 (1.034)	2.469 (2.452)	–	3.055 (3.050)	–
TI-I_4	1.246 (1.244)	1.420 (1.417)	1.276 (1.275)	1.689 (1.683)	1.380 (1.365)	1.058 (1.051)	2.513 (2.465)	–	3.079 (3.061)	–
TI-I_6	1.247 (1.247)	1.419 (1.417)	1.276 (1.276)	1.716 (1.711)	1.370 (1.356)	1.043 (1.035)	–	–	2.925 (2.920)	–
TI-I_7	1.244 (1.243)	1.423 (1.421)	1.275 (1.273)	1.712 (1.706)	1.371 (1.356)	1.057 (1.051)	–	–	2.939	–
TI-I_8	1.243 (1.243)	1.427 (1.426)	1.273 (1.272)	1.720 (1.715)	1.370 (1.355)	1.043 (1.036)	–	–	–	–
TI-I_9	1.241 (1.240)	1.436 (1.240)	1.272 (1.267)	1.712 (1.702)	1.371 (1.356)	1.053 (1.046)	2.352 (2.192)	–	4.440 (4.409)	–
TI-I_{10}	1.250 (1.250)	1.416 (1.416)	1.277 (1.275)	1.706 (1.704)	1.371 (1.355)	1.041 (1.034)	–	–	–	–
TI-I_{11}	1.247 (1.244)	1.421 (1.421)	1.275 (1.273)	1.704 (1.702)	1.372 (1.356)	1.056 (1.051)	–	–	–	–
TI-I_{12}	1.243 (1.243)	1.426 (1.425)	1.273 (1.271)	1.700 (1.691)	1.387 (1.371)	1.043 (1.035)	–	–	–	–
TI-I_{13}	1.241 (1.240)	1.435 (1.440)	1.271 (1.269)	1.693 (1.686)	1.386 (1.370)	1.053 (1.047)	–	–	–	–
TI-I_{14}	1.250 (1.250)	1.415 (1.414)	1.276 (1.274)	1.686 (1.680)	1.389 (1.372)	1.041 (1.034)	–	–	–	–
TI-I_{15}	1.247 (1.244)	1.420 (1.419)	1.274 (1.271)	1.685 (1.678)	1.389 (1.372)	1.056 (1.051)	–	–	–	–
T-A_1	1.284 (1.292)	1.345 (1.338)	1.333 (1.339)	1.645 (1.637)	–	1.032 (1.032)	–	2.167 (2.137)	2.956 (2.940)	–
T-A_2	1.286 (1.305)	1.326 (1.309)	1.342 (1.359)	1.632 (1.613)	–	1.031 (1.020)	–	–	3.033 (3.020)	–
T-A_3	1.285 (1.298)	1.337 (1.326)	1.332 (1.343)	1.630 (1.617)	–	1.027 (1.020)	–	–	–	–
T-A_4	1.288 (1.304)	1.328 (1.313)	1.334 (1.347)	1.633 (1.617)	–	1.030 (1.020)	–	–	–	–
T-I_1	1.205 (1.215)	1.579 (1.545)	1.406 (1.419)	1.603 (1.591)	–	1.050 (1.037)	–	–	2.660 (2.790)	–
T-I_2	1.234 (1.232)	1.475 (1.473)	1.445 (1.447)	1.578 (1.577)	–	1.057 (1.050)	–	–	2.927 (2.928)	–
T-I_3	1.237 (1.237)	1.469 (1.470)	1.445 (1.446)	1.579 (1.579)	–	1.045 (1.037)	–	–	2.927 (2.921)	–
T-I_4	1.232 (1.229)	1.495 (1.505)	1.437 (1.434)	1.574 (1.575)	–	1.049 (1.044)	2.189 (2.169)	–	–	2.724 (2.712)
T-I_5	1.231 (1.229)	1.489 (1.493)	1.444 (1.443)	1.576 (1.576)	–	1.056 (1.050)	–	–	–	–
T-I_6	1.235 (1.236)	1.478 (1.475)	1.450 (1.453)	1.575 (1.574)	–	1.044 (1.036)	–	–	–	–

cc-pVTZ, MP2/6-311++G**, and G2MP2) and DFT (B3LYP/aug-cc-pVTZ and B3LYP/6-311++G**) calculations and harmonic vibrational frequencies also calculated to confirm the nature of the stationary points found and to discuss the ZPVE correction. The NBO and AIM analyses were used to discuss the origin of conformational preference and hydrogen-bond strength. Theoretical calculations show that TI-I is the most stable conformer of TNMH both in the gas phase and in solution. We concluded that the hydrogen-bond strength in TI-I_2, TI-I_3, TI-I_4, TI-I_5, TI-I_9, T-A_1, and T-I_4 conformers in water and CCl_4 solution is weaker than in the gas phase.

Table 9 Stability order (SO) and relative energies (RE) of TI-I, T-A, and T-I conformers at various computational methods (kcal/mol) in water and CCl_4 solutions

Water				CCl_4			
B3LYP		MP2		B3LYP		MP2	
SO	RE	SO	RE	SO	RE	SO	RE
$TI\text{-}I_{10}$	0.00	$TI\text{-}I_{10}$	0.00	$TI\text{-}I_{10}$	0.00	$TI\text{-}I_{10}$	0.00
$TI\text{-}I_{14}$	0.12	$TI\text{-}I_{14}$	0.21	$TI\text{-}I_{6}$	0.13	$TI\text{-}I_{6}$	0.19
$T\text{-}A_{4}$	0.49	$TI\text{-}I_{6}$	1.03	$TI\text{-}I_{14}$	0.83	$TI\text{-}I_{14}$	0.91
$TI\text{-}I_{6}$	0.99	$TI\text{-}I_{3}$	2.44	$TI\text{-}I_{3}$	1.04	$TI\text{-}I_{3}$	1.42
$TI\text{-}I_{3}$	2.17	$TI\text{-}I_{2}$	2.71	$T\text{-}A_{3}$	2.00	$TI\text{-}I_{1}$	3.01
$T\text{-}A_{3}$	2.75	$TI\text{-}I_{11}$	3.22	$TI\text{-}I_{1}$	2.86	$TI\text{-}I_{8}$	3.80
$TI\text{-}I_{11}$	2.80	$TI\text{-}I_{15}$	3.36	$T\text{-}A_{4}$	3.47	$TI\text{-}I_{12}$	4.85
$TI\text{-}I_{15}$	2.95	$TI\text{-}I_{8}$	3.60	$TI\text{-}I_{8}$	4.35	$TI\text{-}I_{7}$	4.98
$TI\text{-}I_{7}$	3.62	$TI\text{-}I_{12}$	3.82	$TI\text{-}I_{7}$	4.40	$TI\text{-}I_{11}$	5.44
$TI\text{-}I_{1}$	4.13	$TI\text{-}I_{7}$	3.99	$TI\text{-}I_{11}$	4.84	$TI\text{-}I_{9}$	5.50
$TI\text{-}I_{8}$	4.16	$TI\text{-}I_{1}$	4.41	$T\text{-}A_{1}$	4.99	$TI\text{-}I_{4}$	5.83
$TI\text{-}I_{12}$	4.27	$TI\text{-}I_{4}$	5.55	$TI\text{-}I_{4}$	5.03	$T\text{-}A_{3}$	6.19
$TI\text{-}I_{4}$	4.93	$TI\text{-}I_{9}$	5.59	$TI\text{-}I_{12}$	5.28	$TI\text{-}I_{13}$	6.40
$TI\text{-}I_{9}$	5.89	$TI\text{-}I_{13}$	5.81	$TI\text{-}I_{15}$	5.96	$TI\text{-}I_{15}$	6.63
$TI\text{-}I_{13}$	6.08	$T\text{-}A_{4}$	7.41	$TI\text{-}I_{9}$	6.04	$TI\text{-}I_{2}$	6.95
$T\text{-}A_{2}$	6.13	$T\text{-}A_{3}$	8.53	$TI\text{-}I_{2}$	6.34	$T\text{-}A_{1}$	7.92
$T\text{-}A_{1}$	6.31	$T\text{-}A_{1}$	9.42	$TI\text{-}I_{13}$	6.53	$T\text{-}A_{4}$	8.44
$TI\text{-}I_{2}$	8.67	$T\text{-}A_{2}$	11.96	$T\text{-}A_{2}$	9.21	$T\text{-}A_{2}$	12.49
$T\text{-}I_{1}$	27.57	$T\text{-}I_{1}$	14.67	$T\text{-}I_{1}$	26.58	$T\text{-}I_{1}$	21.19
$T\text{-}I_{6}$	28.61	$T\text{-}I_{6}$	24.22	$T\text{-}I_{3}$	27.03	$T\text{-}I_{3}$	22.55
$T\text{-}I_{3}$	29.17	$T\text{-}I_{3}$	24.50	$T\text{-}I_{6}$	27.46	$T\text{-}I_{6}$	22.66
$T\text{-}I_{5}$	31.63	$T\text{-}I_{5}$	27.34	$T\text{-}I_{4}$	29.43	$T\text{-}I_{4}$	26.04
$T\text{-}I_{4}$	31.72	$T\text{-}I_{4}$	27.85	$T\text{-}I_{5}$	31.30	$T\text{-}I_{5}$	27.55
$T\text{-}I_{2}$	32.31	$T\text{-}I_{2}$	28.45	$T\text{-}I_{2}$	32.17	$T\text{-}I_{2}$	27.91

References

1. Schessl HW (1995) In: Othmer K (ed) Encyclopedia of chemical technology, vol 13. Wiley, New York
2. Golabi SM, Zare HR (1999) J Electroanal Chem 465:168–176
3. Poso A, Wright Av, Gynther J (1995) Mutat Res 332:63–71
4. Choudhary G, Hansen H (1998) Chemosphere 37:801–843
5. Korfhage KM, Ravichandran K, Baldwin RP (1984) Anal Chem 56:1514–1517
6. Nguyen HP, Seto NOL, Cai Y, Leinala EK, Borisova SN, Palcic MM, Evans SV (2003) Biol J Chem 278:49191–49195
7. Song Y, Zhang W, Ji H, Zhou Y, Zhu J, Lu J (2001) Zhongguo Yaowu Huaxue Za Zhi 11:311–316
8. Hobza P, Havlas Z (2000) Chem Rev 100:4253–4264
9. Raissi H, Yoosefian M, Hajizadeh A, Imampour JS, Karimi M, Farzad F (2012) Bull Chem Soc Jpn 85:87–92
10. Wysokinski R, Biennko DC, Michalska D, Huyskens TZ (2005) Chem Phys 315:17–26
11. Raissi H, Yoosefian M, Zamani S, Farzad F (2012) J Sulfur Chem 33:75–85
12. Krygowski TM, Steüpien BT (2005) Chem Rev 105:3482–3512 (and references therein)
13. Raissi H, Jalbout AF, Yoosefian M, Fazli M, Nowroozi A, Shahini M, Leon A (2010) Int J Quant Chem 110:821–830
14. Lammermann A, Szatmari I, Fulop F, Kleinpeter E (2009) J Phys Chem A 113:6197–6205
15. Raissi H, Yoosefian M, Mollania F, Farzad F, Nowroozi AR, Loghmaninejad D (2011) Comput Theor Chem 966:299–305
16. Raissi H, Yoosefian M, Mollania F (2012) Int J Quant Chem 112:2782–2786
17. Raissi H, Yoosefian M, Khoshkhou SJ (2012) Comput Theor Chem 983:1–6
18. Koch U, Popelier PLA (1995) J Phys Chem 99:9747–9754
19. Gilli G, Bellucci F, Ferretti V, Bertolasi V (1989) J Am Chem Soc 111:1023–1028
20. Bertolasi V, Gilli P, Ferretti V, Gilli G (1991) J Am Chem Soc 113:4917–4925
21. Gilli P, Bertolasi V, Pretto L, Ferretti V, Gilli G (2004) J Am Chem Soc 126:3845–3855
22. Espinosa E, Molins E (2000) J Chem Phys 113:5686–5694
23. Frisch MJ, Trucks GW, Schlegel HB, Scuseria GE, Robb MA, Cheeseman JR, Zakrzewski VG, Montgomery JA, Stratmann JRE, Burant JC, Dapprich S, Millam JM, Daniels AD, Kudin KN, Strain MC, Farkas O, Barone V, Cossi M, Cammi R, Mennucci B, Pomelli C, Adamo C, Clifford S, Ochterski J, Petersson GA, Ayala PY, Cui Q, Morokuma K, Malick DK, Rabuck AD, Raghavachari K, Foresman JB, Cioslowski J, Ortiz JV, Stefanov BB, Liu G, Liashenko A, Piskorz P, Komaromi I, Gomperts R, Martin RL, Fox DJ, Keith T, Al-Laham MA, Peng CY, Nanayakkara A, Gonzalez C, Challacombe M, Gill PMW, Johnson B, Chen W, Wong MW, Andres JL, Gonzalez C, Head-Gordon M, Replogle ES, Pople JA (1998) Gaussian 98, revision A.7. Gaussian, Inc, Pittsburgh
24. Becke AD (1993) J Chem Phys 98:5648–5652
25. Møller C, Plesset MS (1934) Phys Rev 46:618–622
26. Kendall RA, Dunning TH, Harrison RJ (1992) J Chem Phys 96:6796–6806
27. Bader RFW (1998) J Phys Chem A 102:7314–7323
28. Glendening DE, Reed AE, Carpenter JE, Weinhold F (1996) NBO, Version 3.1. Gaussian, Inc., Pittsburgh
29. Wendt M, Weinhold F (2001) NBOView 1.0. Theoretical Chemistry Institute, University of Wisconsin, Madison
30. Tomasi J, Cammi R, Mennucci B, Cappelli C, Corni S (2002) Phys Chem Chem Phys 4:5697–5712
31. Cyranski MK, Krygowski TM, Katritzky AL, Schleyer PvR (2002) J Org Chem 67:1333–1338
32. Mrozek A, Karolak-Wojciechowska J, Amiel P, Barbe J (2000) J Mol Struct 524:159–167
33. Poater J, Duran M, Sola M, Silvi B (2005) Chem Rev 105: 3911–3947
34. Matito E, Durán M, Solà M (2005) J Chem Phys 122: 014109–014117
35. Wolinski K, Hinton JF, Pulay P (1990) J Am Chem Soc 112: 8251–8260
36. Krygowski TM, Cyranski MK (2001) Chem Rev 101:1385–1419
37. Grabowski SJ (2007) J Mol Struct (THEOCHEM) 811:61–67
38. Durig JR, Little TS, Gounev TK, Gardner JK, Sullivan JF (1996) J Mol Struct 375:83–94
39. Eliel EL, Wilen SH (1994) Stereochemistry of organic compounds. Wiley, New York
40. Kemp JD, Pitzer KS (1936) J Chem Phys 4:749–753
41. Pitzer KS (1952) Discuss Faraday Soc 10:66–93